Adatom dynamics and the surface reconstruction of Si(110) revealed using time-resolved electron microscopy

Tom Furnival,[1] Daniel Knez,[2,3,a)] Eric Schmidt,[1] Rowan K. Leary,[1] Gerald Kothleitner,[2,3] Ferdinand Hofer,[2,3] Paul D. Bristowe,[1] and Paul A. Midgley[1,a)]

[1)] *Department of Materials Science & Metallurgy, University of Cambridge, 27 Charles Babbage Road, Cambridge CB3 0FS, United Kingdom*

[2)] *Institute for Electron Microscopy and Nanoanalysis (FELMI), Graz University of Technology, Steyrergasse 17, 8010 Graz, Austria*

[3)] *Graz Centre for Electron Microscopy (ZFE), Steyrergasse 17, 8010 Graz, Austria*

(Dated: 4 October 2018)

Surface dynamics lie at the heart of many areas of materials and chemical science, including heterogeneous catalysis, epitaxial growth and device fabrication. Characterizing the dynamics of surface adsorption, reactions and diffusion at the atomic scale is crucial to understanding and controlling such processes. Here we use aberration-corrected scanning transmission electron microscopy to analyze the diffusive behavior of Pt atoms adsorbed on the Si(110) surface, and characterize the effects of the electron beam on adatom motion, including a bias introduced by the raster scan of the probe. We further observe the evolution of the Si(110) surface, revealing evidence of developing surface steps attributed to the 16×2 surface reconstruction. These results demonstrate a framework for studying complex atomic-scale surface dynamics using aberration-corrected electron microscopy.

The silicon surface is one of the most widely-studied due to its importance in the semiconductor industry, and in particular the growth of oxide and metal films for metal–oxide–semiconductor field-effect transistors (MOSFETs). Direct imaging of the surface is typically performed using scanning tunneling microscopy (STM), which has revealed long-range reconstructions such as the Si(111)-7×7 surface[1], or else the structures and properties are inferred from diffraction or spectroscopic techniques. The clean Si(110) surface is known to exhibit a similarly long-range 16×2 reconstruction, with steps and terraces running in ⟨112⟩ directions[2]. Theoretical calculations using density functional theory (DFT) have indicated that pairs of Si pentagons arranged into zigzag chains are integral to the stability of this surface[3,4]. Further investigations of the oxidation behavior point to preferential growth in the ⟨112⟩ direction, with oxygen atoms clustering at these pentagonal pairs during the early stages of oxidation[5–7]. The stability of the surface is also heavily influenced by the presence of metal adatoms, and the diffusive behavior of these atoms is important in the initial stages of metal silicide film growth[8]. An atomic-scale understanding of these dynamic processes is therefore fundamental to the design and engineering of surface systems.

While *in situ* STM studies can be performed at high temperatures and at frame rates of 10 s^{-1} or higher[9], the hardware challenges are significant, and the achievable resolution can often degrade over time[10]. An alternative tool with comparable temporal and spatial resolution is aberration-corrected scanning transmission electron microscopy (STEM), which facilitates further characterization through quantitative imaging and atom-by-atom spectroscopy[11,12]. Time-resolved experiments using STEM typically employ the electron beam to excite and subsequently record dynamic behavior at the atomic scale. Examples include observations of atomic motion in graphene[13], on surfaces[14], and in bulk materials[15]. Combined with developments in environmental STEM[16] for *in situ* imaging, time-resolved STEM is an extremely promising technique for surface studies with single atom sensitivity. Recently, cross-sectional imaging has been used to analyze the surface reconstruction of clean $SrTiO_3$ at elevated temperatures[17]. However, to fully realize its potential as an *in situ* characterization technique requires an understanding of the beam–specimen interaction, and in particular the effect the beam has on atomic motion. Furthermore, computational processing methods are becoming increasingly important as temporal datasets grow in both size and complexity.

In this Letter we use aberration-corrected STEM to probe the reconstruction of the Si(110) surface as well as the dynamic behavior of Pt adatoms. Using the electron beam to excite the adatoms, we apply image processing algorithms to separate the dynamics of the substrate from the adatoms, which we then analyze independently. Molecular dynamics (MD) simulations are performed to explore the distinctive surface features observed in the substrate, while automated particle tracking enables analysis of the diffusive motion of the Pt adatoms.

A thin Si lamella was prepared from a monocrystalline wafer using focused ion beam (FIB) milling, and Pt atoms were deliberately sputtered across the Si surface during this process (see Supplementary Material for details). Annular dark-field (ADF) STEM imaging was performed on an FEI Titan[3] (S)TEM operating at a pri-

[a)] To whom all correspondence should be addressed. daniel.knez@felmi-zfe.at, pam33@cam.ac.uk

mary beam energy of 300 keV[18]. Image sequences were acquired at a rate of 4 frames s^{-1}, which is sufficient to track the movement of the adatoms with an estimated dose rate of 2×10^6 e^- nm^{-2} s^{-1}. The high accelerating voltage in this experiment will induce changes in both the substrate and the adatoms due to elastic collisions between the energetic electrons and the Coulomb field of the atomic nuclei. Such interactions can be isolated to be the prevalent cause of beam induced sample changes in metals and many semiconductors[19]. The maximum transferable momentum during an elastic scattering event is sufficient to displace adatoms out of stable binding sites, leading to motion across the surface until another stable site is encountered. For weakly bound (surface) atoms even sputtering can occur[20,21]. In contrast, inelastic scattering events such as ionization and excitation, are equilibrated fast enough to prevent a mechanical response of an atom in sufficiently conducting materials like Si under present conditions[19,22]. Hence, effects of beam induced heat and charge accumulation can be neglected in our case.

The image sequences were initially denoised with the PGURE-SVT algorithm[23], which uses singular value thresholding to exploit spatio-temporal correlations in small image patches. Figure 1a shows an as-acquired frame from one of the sequences, and the processed frame is shown in Figure 1b for comparison. Following the denoising, the image sequences were aligned using a non-rigid registration algorithm designed for STEM imaging[24]. While PGURE-SVT exploits local correlations to filter noise in an unaligned image sequence, the subsequent alignment means the global correlations of the Si lattice can then be utilized for further processing. This is achieved using robust principal component analysis (RPCA)[25]. The frames are stacked into columns of a matrix, which is then modelled as the sum of two components. One is a low-rank matrix, here corresponding to the temporally correlated Si lattice, and the other is a sparse "error" component, relating to the relatively uncorrelated mobile adatoms. Here we use an online RPCA algorithm to track small changes in the low-rank component over time[26]. Figures 1c,d show the results of the RPCA processing, with the Si lattice and Pt adatoms clearly separated (Multimedia View). Any changes in the substrate can now be analyzed independently of the diffusive adatom behaviour.

We first investigate the dynamic behaviour of the Pt adatoms on the Si surface by looking at the sparse component of the RPCA decomposition (Fig. 1d). At the experimental accelerating voltage of 300 kV, a collision with an electron can impart up to 4.5 eV to a Pt atom[20], which will be more than sufficient to excite the adsorbed atom out of a surface site and thus diffuse over the surface. Here the length of the sequence and the clear separation of the substrate and adatoms using RPCA opens up the opportunity to perform automated particle detection and tracking, in a manner similar to established fluorescence microscopy techniques[27].

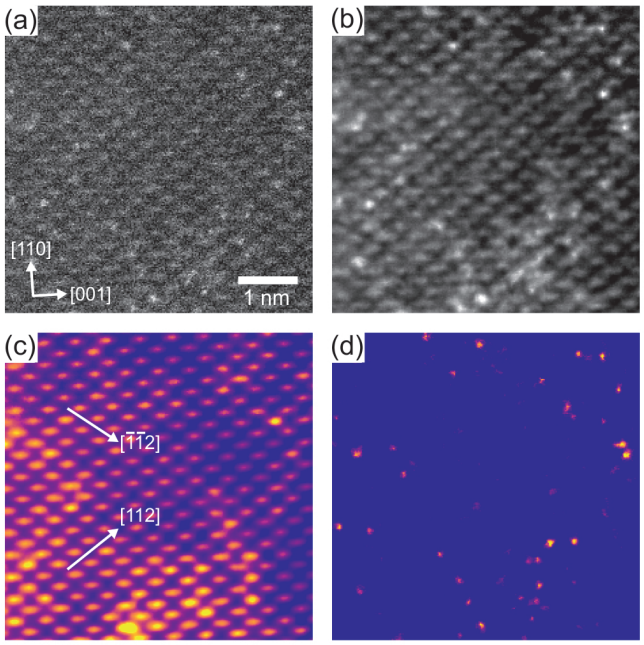

FIG. 1. (a) A frame from an ADF-STEM sequence of Pt adatoms on Si(110). (b) The same frame following processing to remove noise. (c) The low-rank component recovered by RPCA processing. (d) The sparse component containing the Pt adatoms after applying RPCA. (Multimedia View)

A wavelet-based feature detector was used to extract the approximate positions of the adatoms from sequence 1, which were further refined by fitting 2D Gaussians to a small window around each atom. The positions were then combined into trajectories using a reinforcement learning approach to particle tracking (see Supplementary Material for details); in total, 309 particle tracks were analyzed with lengths of 2–56 s. The mean-squared displacement (MSD) of the trajectories is seen to be linear in time (Fig. 2a), which indicates that the Pt adatoms are undergoing a normal diffusion process as a result of the beam-induced motion. This finding is in contrast to the anomalous diffusion of Cu on graphene oxide reported recently[28]. Note that at long times the noise in the MSD increases due to a smaller number of trajectories available for averaging.

Analysis of the magnitude and direction of the atom displacements in Figure 2b reveals a preference for left-to-right adatom jumps in approximately the [001] direction. Figure 2b plots the probability of a displacement, $P(\Delta x, \Delta y)$, weighted by the magnitude to give additional importance to long jumps (which are likely beam-driven) and reduce the influence of very small displacements (likely caused by measurement error or particles staying in place). Two important points can be drawn from this plot. The first is that there is a preference for jumps in line with the Si dumbbells, which are tilted a few degrees off the horizontal axis (cf. Fig. 1). Figures 2c,d overlay two of the adatom trajectories on the substrate

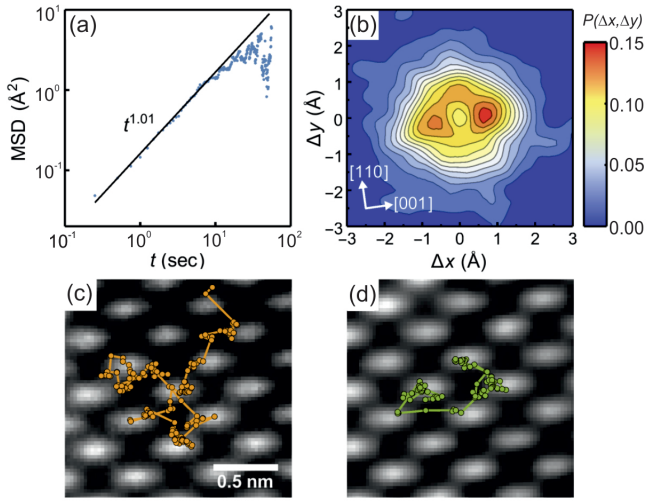

FIG. 2. (a) MSD of the atom trajectories extracted from the ADF-STEM sequence. The best-fit line is shown in black along with the fitted exponent. (b) The probability of adatom displacements, $P(\Delta x, \Delta y)$, weighted by the displacement magnitude. (c,d) Two of the Pt adatom tracks overlaid onto the background image of the Si lattice (Fig. 1c).

image extracted with RPCA (Fig. 1c), and show that there is a tendency for the adatom to sit atop a dumbbell rather than off it, although the image resolution is insufficient to elucidate the complete local structure. On the reconstructed surface one Si atom of the pair will sit higher than the other, potentially providing a stable site for the Pt atom. The role of oxygen atoms in binding the Pt to the substrate cannot be ruled out either, and although DFT calculations could resolve this ambiguity over stable sites, the size and complexity of the (oxidized) surface reconstruction and the beam-induced changes make this a potentially challenging computation.

The second observation from Figure 2b is the preference for jumps in the [001] direction. This is in the fast scan direction of the STEM probe, suggesting that the adatoms are, in effect, being "pushed" by the electron beam. The aberration-corrected probe resembles an Airy pattern[29] with an estimated full-width half-maximum of 1.2 Å of the central disc. In comparison, the experimental pixel size is 0.24 Å, meaning that a significant fraction of the electron dose will fall outside the pixel being imaged. The large probe tails thus increase the likelihood of an adatom being displaced when the probe is nearby[30]. Since the probe will always approach the Pt adatom from the left in this experiment, we suggest that this contributes to the directional bias, and therefore the scan direction is another important consideration for *in situ* studies of adatom dynamics, alongside aspects such as accelerating voltage, beam current and dwell time. Understanding the relationships between beam effects and the underlying physical process is crucial for a full characterization of surface dynamics, and future experiments that vary the scan direction, for example between individual frames as in the RevSTEM technique[31], may shed further light on the origins of the directional bias observed in Figure 2b.

We now turn our attention to the low-rank component of the RPCA decomposition. Figure 1c exhibits several bright chevron-like features on the Si surface running in ⟨112⟩-type directions. These features are even clearer in Figure 3a,b (Multimedia view), where the Si atomic columns are resolved into distinct dumbbells (spacing 1.36 Å, Fig. 3e). The ⟨112⟩ direction is particularly significant, since it is both the direction of the steps on the clean 16×2 reconstruction, and also the preferred growth direction for oxide formation on Si(110)[5]. Determining the exact origin of these features is thus important for understanding how the beam is affecting the substrate, especially as the features are seen to move and become sharper and brighter over the course of the sequence. The line profiles in Figure 3e show that early in the sequence the chevron features are only just visible, but after 45 s of acquisition there is a clear change in the intensity of neighbouring Si dumbbells.

One of the advantages of ADF imaging is that the scattered intensity scales with the thickness and the atomic number, Z, as $Z^{\sim 1.7}$[11]. This facilitates elemental characterization and atom counting with atomic resolution, as well as direct comparison with theoretical structures and simulated ADF images[32]. Using quantitative ADF imaging, analysis of the intensity of a Si atomic column with a Pt atom atop compared to a bare Si column gave an estimated thickness of the lamella of 7 nm (corresponding to approximately 18 Si atoms in a column). Quantitative analysis can also be used to determine whether the bright ⟨112⟩ features are caused by the Si surface reconstruction or oxidation. Assuming a Z exponent of 1.7, the intensity of a single Si atom is equivalent to approximately 2.5 O atoms. This suggests that the intensity variations are more likely to be caused by Si rather than O atoms, which are expected to be more mobile under the electron beam and thus be blurred out during the image acquisition and processing. It is highly likely that the electron beam will preferentially sputter off oxygen and other low atomic number contaminants, leaving behind a cleaner Si surface[33].

To confirm that the distinct features observed are indeed caused by the Si surface reconstruction and not oxide formation, we performed a series of MD simulations of the oxidation of clean Si, and used simulated STEM images to relate the MD results to the experimental images. The size of the 16×2 reconstruction limits the feasibility of *ab initio* MD simulations. Instead, we carried out classical MD simulations using the reactive force field (ReaxFF) developed specifically for the Si-O system[34], which was designed to bridge the gap between expensive quantum mechanical calculations and empirical classical potentials. We found that ReaxFF successfully describes the DFT-calculated surface reconstruction shown in Figure 3c[4], and that it also replicates the spontaneous dissociation of O_2 into atomic oxygen on the surface of silicon,

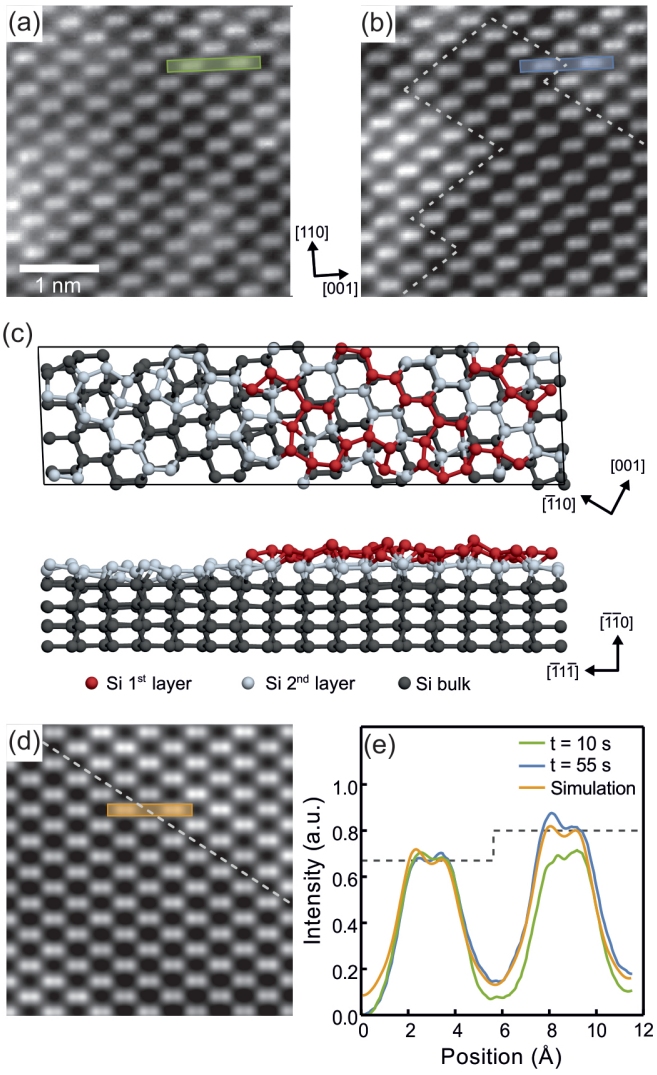

FIG. 3. (a) The low-rank background of an ADF-STEM sequence of Pt adatoms on Si(110) after 10 s. (b) The same region 45 s later. Chevron-like features are indicated by dashed grey lines. (Multimedia view) (c) The 16×2 reconstruction of the Si(110) surface, viewed from above and along the [$\bar{1}$12] direction, with surface Si atoms highlighted. (d) A simulated ADF-STEM image of the structure in (c), with the step running diagonally across the image, indicated by a dashed grey line. (e) Line profiles from the experimental and simulated STEM images in (a), (b) and (d). The dashed grey line indicates the position of the step on the clean surface.

which is the first step in the oxidation process on other low-index surfaces[35]. Details of the MD simulations can be found in the Supplementary Material.

Figure 3d shows a simulated ADF-STEM image of a 7 nm thick slab with a clean, reconstructed Si surface, and line profiles across the step (Fig. 3e) show that the simulation closely matches the observed intensity variations. Adding even a small amount of oxygen (64 atoms or ca. 1 ML coverage) to the surface has a significant effect on the line profiles (see Figure S2 in the Supplementary Information), disrupting the surface reconstruction and obscuring the ⟨112⟩ step. These simulations indicate that the change in height of the Si surface is the major contribution to the image intensity, and that the bright ⟨112⟩ features are indeed caused by the step in the 16×2 reconstruction.

Since STEM is a projected imaging method, it is important to consider that the observed features may exist on both the top and bottom surfaces, making the separation of their contributions to the image intensity difficult. However, sputtering of oxygen by the electron beam is likely to occur preferentially on the bottom surface of the lamella, due to the predominant momentum transfer component parallel to the electron beam. Hence, the oxygen coverage on the top surface is expected to be more stable by comparison. Quantification using electron energy-loss spectroscopy (EELS), furthermore, shows that the oxygen content decreases over time under the electron beam (see Supplementary Material). Combined with the knowledge that the oxidized Si surface does not exhibit the bright ⟨112⟩ features of the clean surface, we conclude that sputtering of oxygen by the electron beam leads to the 16×2 surface reconstruction on the bottom surface only. This is consistent with the behavior seen in the line profiles in Figure 3e. Note that the intensity values in this figure are measured from the low-rank component rather than the raw experimental data. The intensity profile, therefore, lacks a constant background which would otherwise be present.

In conclusion, we have demonstrated an approach to observing and understanding the dynamics of surfaces using atomically-resolved STEM image sequences. By exploiting temporal correlations between frames, we analyzed the dynamics of surface adatoms induced by the electron beam, and further explored the surface reconstruction of Si(110). The methods presented here are widely applicable to the study of atom dynamics with aberration-corrected STEM, and are particularly important for developing *in situ* imaging techniques for surface science. Crucially, combining quantitative ADF imaging with MD simulations maintains both the temporal resolution and the low dose imaging conditions, which are key criteria to observe atomic-scale dynamics.

SUPPLEMENTARY MATERIAL

See Supplemental Material for details of the sample preparation, image processing, MD simulations, particle tracking and EELS analysis, and two movies showing the surface and adatom behaviour.

ACKNOWLEDGMENTS

The research leading to these results has received funding from the European Research Council under the European Union's Seventh Framework Programme

(FP7/2007–2013)/ERC grant agreement 291522–3DIMAGE, as well as from the European Union Seventh Framework Programme under Grant Agreement 312483–ESTEEM2 (Integrated Infrastructure Initiative–I3). R.L. acknowledges a Junior Research Fellowship from Clare College. D.K., G.H. and F.H. would like to thank Martina Dienstleder for help with sample preparation and Johanna Kraxner for helpful discussions.

[1]G. Binnig, H. Rohrer, C. Gerber, and E. Weibel, "7×7 Reconstruction on Si(111) Resolved in Real Space," Phys. Rev. Lett. **50**, 120–123 (1983).

[2]T. An, M. Yoshimura, I. Ono, and K. Ueda, "Elemental structure in Si(110)-(16×2) revealed by scanning tunneling microscopy," Phys. Rev. B **61**, 3006–3011 (2000).

[3]A. A. Stekolnikov, J. Furthmüller, and F. Bechstedt, "Long-Range Surface Reconstruction: Si(110)-(16×2)," Phys. Rev. Lett. **93**, 136104 (2004).

[4]T. Yamasaki, K. Kato, T. Uda, T. Yamamoto, and T. Ohno, "First-principles theory of Si(110)-(16×2) surface reconstruction for unveiling origin of pentagonal scanning tunneling microscopy images," Appl. Phys. Express **9**, 035501 (2016).

[5]H. Togashi, Y. Takahashi, A. Kato, A. Konno, H. Asaoka, and M. Suemitsu, "Observation of Initial Oxidation on Si(110)-16×2 surface by Scanning Tunneling Microscopy," Jpn. J. Appl. Phys. **46**, 3239–3243 (2007).

[6]M. Suemitsu, Y. Yamamoto, H. Togashi, Y. Enta, A. Yoshigoe, and Y. Teraoka, "Initial oxidation of Si(110) as studied by real-time synchrotron-radiation x-ray photomission spectroscopy," J. Vac. Sci. Technol. **27**, 547 (2009).

[7]T. Nagasawa, S. Shiba, and K. Sueoka, "First-principles study on initial stage of oxidation on Si(110) surface," Phys. Status Solidi C **8**, 717–720 (2011).

[8]K. Oura, V. G. Lifshits, A. A. Saranin, A. V. Zotov, and M. Katayama, "Hydrogen interaction with clean and modified silicon surfaces," Surf. Sci. Rep. **35**, 1–69 (1999).

[9]J. Wintterlin, J. Trost, S. Renisch, R. Schuster, T. Zambelli, and G. Ertl, "Real-time STM observations of atomic equilibrium fluctuations in an adsorbate system: O/ru(0001)," Surf. Sci. **394**, 159–169 (1997).

[10]G. Schitter and M. J. Rost, "Scanning probe microscopy at video-rate," Mater. Today **11**, 40–48 (2008).

[11]O. L. Krivanek, M. F. Chisholm, V. Nicolosi, T. J. Pennycook, G. J. Corbin, N. Dellby, M. F. Murfitt, C. S. Own, Z. S. Szilagyi, M. P. Oxley, S. T. Pantelides, and S. J. Pennycook, "Atom-by-atom structural and chemical analysis by annular dark-field electron microscopy," Nature **464**, 571–574 (2010).

[12]Q. M. Ramasse, C. R. Seabourne, D.-M. Kepaptsoglou, R. Zan, U. Bangert, and A. J. Scott, "Probing the Bonding and Electronic Structure of Single Atom Dopants in Graphene with Electron Energy Loss Spectroscopy," Nano Lett. **13**, 4989–4995 (2013).

[13]T. Susi, J. Kotakoski, D. Kepaptsoglou, C. Mangler, T. C. Lovejoy, O. L. Krivanek, R. Zan, U. Bangert, P. Ayala, J. C. Meyer, and Q. M. Ramasse, "Silicon–Carbon Bond Inversions Driven by 60-keV Electrons in Graphene," Phys. Rev. Lett. **113**, 115501 (2014).

[14]P. E. Batson, "Motion of Gold Atoms on Carbon in the Aberration-Corrected STEM," Microsc. Microanal. **14**, 89–97 (2008).

[15]R. Ishikawa, R. Mishra, A. R. Lupini, S. D. Findlay, T. Taniguchi, S. T. Pantelides, and S. J. Pennycook, "Direct Observation of Dopant Atom Diffusion in a Bulk Semiconductor Crystal Enhanced by a Large Size Mismatch," Phys. Rev. Lett. **113**, 1555051 (2014).

[16]E. D. Boyes and P. L. Gai, "Visualising reacting single atoms under controlled conditions: Advances in atomic resolution in situ Environmental (Scanning) Transmission Electron Microscopy (E(S)TEM)," C. R. Phys. **15**, 200–213 (2014).

[17]W. Xu, P. C. Bowes, E. D. Grimley, D. L. Irving, and J. M. LeBeau, "In-situ real-space imaging of single crystal surface reconstructions via electron microscopy," Applied Physics Letters **109**, 201601 (2016).

[18]The beam convergence semi-angle was 19.7 mrad, and the ADF detector angle range was 62–214 mrad. The probe current was 80 pA and the pixel dwell time was 3 μs. Vacuum pressure in the sample chamber was at approximately 10^{-5} Pa.

[19]N. Jiang, "Electron beam damage in oxides: a review," Reports on progress in physics. Physical Society (Great Britain) **79**, 016501 (2016).

[20]R. Egerton, "Beam-Induced Motion of Adatoms in the Transmission Electron Microscope," Microsc. Microanal. **19**, 479–486 (2013).

[21]D. Knez, M. Schnedlitz, M. Lasserus, A. Schiffmann, W. E. Ernst, and F. Hofer, "Modelling electron beam induced dynamics in metallic nanoclusters," Ultramicroscopy **192**, 69–79 (2018).

[22]X. Qu and Q. Deng, "Damage and recovery induced by a high energy e-beam in a silicon nanofilm," RSC Advances **7**, 37032–37038 (2017).

[23]T. Furnival, R. K. Leary, and P. A. Midgley, "Denoising time-resolved microscopy image sequences with singular value thresholding," Ultramicroscopy **178**, 112–124 (2017).

[24]B. Berkels, P. Binev, D. A. Blom, W. Dahmen, R. C. Sharpley, and T. Vogt, "Optimized imaging using non-rigid registration," Ultramicroscopy **138**, 46–56 (2014).

[25]E. J. Candès, X. Li, Y. Ma, and J. Wright, "Robust principal component analysis?" J. ACM **58**, 1–37 (2011).

[26]J. Feng, H. Xu, and S. Yan, "Online robust pca via stochastic optimization," in ***Advances in Neural Information Processing Systems 26***, edited by C. J. C. Burges, L. Bottou, M. Welling, Z. Ghahramani, and K. Q. Weinberger (Curran Associates, Inc., 2013) pp. 404–412.

[27]N. Chenouard, I. Smal, F. de Chaumont, M. Maška, I. F. Sbalzarini, Y. Gong, J. Cardinale, C. Carthel, S. Coraluppi, M. Winter, A. R. Cohen, W. J. Godinez, K. Rohr, Y. Kalaidzidis, L. Liang, J. Duncan, H. Shen, Y. Xu, K. E. G. Magnusson, J. Jaldén, H. M. Blau, P. Paul-Gilloteaux, P. Roudot, C. Kervrann, F. Waharte, J.-Y. Tinevez, S. L. Shorte, J. Willemse, K. Celler, G. P. van Wezel, H.-W. Dan, Y.-S. Tsai, C. Ortiz de Solórzano, J.-C. Olivo-Marin, and E. Meijering, "Objective comparison of particle tracking methods," Nature methods **11**, 281–289 (2014).

[28]T. Furnival, R. K. Leary, E. C. Tyo, S. Vajda, Q. M. Ramasse, J. M. Thomas, P. D. Bristowe, and P. A. Midgley, "Anomalous diffusion of single metal atoms on a graphene oxide support," Chemical Physics Letters **683**, 370–374 (2017).

[29]D. B. Williams and C. B. Carter, "Transmission electron microscopy: A textbook for materials science," (2009).

[30]J. Kotakoski, C. Mangler, and J. C. Meyer, "Imaging atomic-level random walk of a point defect in graphene," Nature Communications **5** (2014).

[31]X. Sang and J. M. LeBeau, "Revolving scanning transmission electron microscopy: Correcting sample drift distortion without prior knowledge," Ultramicroscopy **138**, 28–35 (2014).

[32]J. M. LeBeau, S. D. Findlay, L. J. Allen, and S. Stemmer, "Quantitative Atomic Resolution Scanning Transmission Electron Microscopy," Phys. Rev. Lett. **100**, 206101 (2008).

[33]G. S. Chen, C. B. Boothroyd, and C. J. Humphreys, "Electron-beam-induced damage in amorphous sio$_2$ and the direct fabrication of silicon nanostructures," Philos. Mag. A **78**, 491–506 (1998).

[34]A. D. Kulkarni, D. G. Truhlar, S. G. Srinivasan, A. C. T. van Duin, P. Norman, and T. E. Schwartzentruber, "Oxygen Interactions with Silica Surfaces: Coupled Cluster and Density Functional Investigation and the Development of a New ReaxFF Potential," J. Phys. Chem. C **117**, 258–269 (2013).

[35]L. C. Ciacchi and M. C. Payne, "First-Principles Molecular-Dynamics Study of Native Oxide Growth on Si(001)," Phys. Rev. Lett. **95**, 196101 (2005).